

Diffractive production and the total cross section in deep inelastic scattering*

Masaaki Kuroda

Institute of Physics, Meiji-Gakuin University
Yokohama 244, Japan
and

Dieter Schildknecht

Fakultät für Physik, Universität Bielefeld
D-33501 Bielefeld, Germany

Abstract

We explore the consequences for diffractive production, $\gamma^*p \rightarrow Xp$, in deep inelastic scattering at low values of $x \cong Q^2/W^2 \ll 1$ that follow from our recent representation of the total photoabsorption cross section, σ_{γ^*p} , in the generalized vector dominance/color dipole picture (GVD/CDP) that is based on the generic structure of the two-gluon exchange from QCD. Sum rules are derived that relate the transverse and the longitudinal (virtual) photoabsorption cross section to diffractive forward production of $q\bar{q}$ -states that carry photon quantum numbers (“elastic diffraction”). Agreement with experiment in the W^2 and Q^2 dependence is found for $M_X^2/Q^2 \ll 1$, where M_X is the mass of the produced system X . An additional component (“inelastic diffraction”), not actively contributing to the forward Compton amplitude, is needed for diffractive production at high values of M_X . Our previous theoretical representation of the total photoabsorption cross section, $\sigma_{\gamma^*p} = \sigma_{\gamma^*p}(\eta)$, in terms of the scaling variable $\eta \equiv (Q^2 + m_0^2)/\Lambda^2(W^2)$ is extended to include the entire kinematic domain, $x \leq 0.1$ and all Q^2 with $Q^2 \geq 0$, where scaling in η holds experimentally.

* Supported by the BMBF, Contract 05 HT9PBA2 and by the Ministry of Education, Science and Culture in Japan under the Grant-in-Aid No.14340081.

I. INTRODUCTION

Any theory of diffractive production, $\gamma^*p \rightarrow Xp$ in deep inelastic scattering (DIS), at low $x = Q^2/W^2 \ll 1$ has to discriminate between, and take into account two distinctly different components, an “elastic” and an “inelastic” one. The elastic component, by definition, consists of all and only those final states X that carry the quantum numbers of the photon. Accordingly, the (imaginary) elastic diffractive production amplitude is responsible for the (virtual) forward Compton scattering amplitude that, via the optical theorem, represents the total photoabsorption cross section, $\sigma_{\gamma^*p}(W^2, Q^2)$. The inelastic component contains hadronic states X that do not carry photon quantum numbers. In particular, the inelastic component contains states X of spins different from the spin of one unit carried by the photon. It, obviously, does not contribute to the Compton forward scattering amplitude.

Direct evidence for an inelastic component in diffractive production in DIS is provided by the experimentally observed properties of the hadronic state in diffractive DIS. The thrust and sphericity distributions of the state X are approximately identical [1] to the ones observed in $e^+e^- \rightarrow q\bar{q} \rightarrow$ hadrons. The strong alignment of the jet axis of the $(q\bar{q})$ state X in its rest frame with respect to the virtual photon direction, however, is different from the $1 + \cos^2\theta$ dependence observed in e^+e^- annihilation, and this difference provides evidence for the presence of higher spin states in the system X . Also, in hadron-hadron interactions, diffractive production of states, different in spin from the initial beam particles, is a common feature. The change in spin is connected with a change in parity that obeys the natural-spin-parity connection, $(-1)^{\Delta J}$, [2].

In the present investigation, we consider elastic diffraction in its connection with the total virtual photoabsorption cross section. In terms of the virtual forward Compton scattering amplitude, DIS at low x corresponds to diffractive scattering of the hadronic $(q\bar{q})$ states the photon fluctuates into, as conjectured by generalized vector dominance [3] a long time ago. The $q\bar{q}$ states the photon is coupled to interact via two-gluon exchange [4] with the target nucleon. The $q\bar{q}$ states form a color dipole, and the forward scattering amplitude resulting from two-gluon exchange becomes diagonal, when expressed in terms of the (transverse) quark-antiquark separation in position space [5]. When transformed into momentum space, off-diagonal transitions of destructive nature appear with respect to the masses in the propagators of the incoming and outgoing $q\bar{q}$ states, essential for convergence of the whole formalism, as anticipated by off-diagonal generalized vector dominance [6] in the pre-QCD era¹. Our approach [8, 9, 10] to DIS that is based on the generic two-gluon exchange structure and incorporates the empirical scaling of $\sigma_{\gamma^*p}(W^2, Q^2) = \sigma_{\gamma^*p}(\eta(W^2, Q^2))$ with $\eta \equiv (Q^2 + m_0^2)/\Lambda^2(W^2)$, [8], is appropriately called the generalized vector dominance/color-dipole picture (GVD/CDP).

In the present paper we will show that the total cross section, σ_{γ^*p} , at small x can explicitly be represented by a sum rule that contains the elastic diffractive production amplitude integrated over the masses of the diffractively produced states X . The direct connection of σ_{γ^*p} and diffractive production by the sum rule will be seen to suggest an improved expression for $\sigma_{\gamma^*p} = \sigma_{\gamma^*p}(\eta)$ in the GVD/CDP, such that the GVD/CDP covers the full kinematic range where scaling in η was established [8], i.e. $x < 0.1$ with all $Q^2 \geq 0$.

A comparison of the results for elastic diffraction with the experimental data for $\gamma^*p \rightarrow Xp$ reveals the presence of a large excess in high-mass production, i.e. for $\beta \equiv Q^2/(Q^2 + M_X^2) \ll 1$. This excess is to be associated with inelastic diffractive production.

In Section 2, we briefly present the GVD/CDP for σ_{γ^*p} . In Section 3, we describe elastic diffraction. A comparison of the representations in Sections 2 and 3 implies the sum rules of Section 4. The comparison with the experimental data for diffractive production in Section 5 reveals approximate agreement for small diffractively produced masses, i.e. for $\beta \rightarrow 1$, while showing the mentioned excess for $\beta \rightarrow 0$. The improved representation of $\sigma_{\gamma^*p}(\eta)$ is given in Section 6, while Section 7 summarizes our main conclusions.

II. THE VIRTUAL FORWARD COMPTON SCATTERING AMPLITUDE AND σ_{γ^*p}

The virtual forward Compton scattering amplitude at low x , as mentioned, results from the diffractive scattering of $q\bar{q}$ states on the proton,

$$q\bar{q} + \text{proton} \rightarrow q\bar{q} + \text{proton}, \quad (1)$$

where both the incoming and outgoing $q\bar{q}$ pair carry the quantum numbers of the photon. In particular, the incoming and outgoing $q\bar{q}$ states in (1) have spin 1. The $x \rightarrow 0$ limit of the two-gluon-exchange virtual forward Compton

¹ Compare also ref.[7] for a discussion of the relevance of off-diagonal generalized vector dominance

scattering amplitude is embodied [8] in the position-space representation [5] for the transverse and longitudinal parts of the photoabsorption cross section, $\sigma_{\gamma_{T,p}^*}$ and $\sigma_{\gamma_{L,p}^*}$,

$$\sigma_{\gamma_{T,L}^* p}(W^2, Q^2) = \int dz \int d^2 r_\perp \sum_{\lambda, \lambda' = \pm 1} |\psi_{T,L}^{(\lambda, \lambda')}(\vec{r}_\perp, z, Q^2)|^2 \sigma_{(q\bar{q})p}(\vec{r}_\perp^2, z, W^2) \quad (2)$$

with the Fourier representation of the color dipole cross section,

$$\sigma_{(q\bar{q})p}(\vec{r}_\perp^2, z, W^2) = \int d^2 l_\perp \tilde{\sigma}_{(q\bar{q})p}(\vec{l}_\perp^2, z, W^2) (1 - e^{-i\vec{l}_\perp \vec{r}_\perp}) \quad (3)$$

that incorporates color transparency and (hadronic) unitarity [8]. In (2) and (3), we use the conventional notation, in which \vec{r}_\perp denotes the transverse interquark separation and z the fraction of the (virtual) photon momentum carried by the quark. The transverse gluon momentum is denoted by \vec{l}_\perp . The square of the photon wave function reads²

$$\sum_{\lambda, \lambda'} \left| \psi_{T,L}^{(\lambda, \lambda')}(\vec{r}_\perp, z; Q^2) \right|^2 = 3 \cdot \frac{4\pi}{(16\pi^3)^2} \int d^2 k'_\perp \int d^2 k_\perp \mathcal{M}_{T,L}^*(\vec{k}'_\perp, z, Q^2) \mathcal{M}_{T,L}(\vec{k}_\perp, z, Q^2) \exp(i\vec{k}'_\perp - \vec{k}_\perp) \vec{r}_\perp, \quad (4)$$

where

$$\mathcal{M}_T^*(\vec{k}'_\perp, z, Q^2) \cdot \mathcal{M}_T(\vec{k}_\perp, z, Q^2) = \frac{8\pi\alpha(\vec{k}'_\perp \cdot \vec{k}_\perp) \sum_f Q_f^2 (z^2 + (1-z)^2)}{(z(1-z)Q^2 + \vec{k}'_\perp{}^2)(z(1-z)Q^2 + \vec{k}_\perp{}^2)} \quad (5)$$

and

$$\mathcal{M}_L^*(\vec{k}'_\perp, z, Q^2) \cdot \mathcal{M}_L(\vec{k}_\perp, z, Q^2) = \frac{32\pi\alpha Q^2 \sum_f Q_f^2 z^2 (1-z)^2}{(z(1-z)Q^2 + \vec{k}'_\perp{}^2)(z(1-z)Q^2 + \vec{k}_\perp{}^2)}. \quad (6)$$

Substitution of the photon wave function (4) and the dipole cross section (3) into (2) takes us back to the momentum space representation of the photoabsorption cross section

$$\sigma_{\gamma_{T,L}^* p}(W^2, Q^2) = \frac{3}{16\pi^3 \cdot 2} \int dz \int d^2 k_\perp \int d^2 l_\perp \tilde{\sigma}_{(q\bar{q})p}(\vec{l}_\perp^2, z, W^2) \cdot |\mathcal{M}_{T,L}(z, \vec{k}_\perp, Q^2) - \mathcal{M}_{T,L}(z, \vec{k}_\perp + \vec{l}_\perp, Q^2)|^2. \quad (7)$$

Here, \vec{k}_\perp denotes the transverse momentum of the quark in the $q\bar{q}$ state that originates from the (virtual) photon. The two-gluon exchange interaction of the $q\bar{q}$ pair in (7) involves integration over the (transverse) momentum, \vec{l}_\perp , of the gluon. Guided by the empirical scaling law[8],

$$\sigma_{\gamma^* p}(W^2, Q^2) = \sigma_{\gamma^* p}(\eta(W^2, Q^2)), \quad (8)$$

with

$$\eta(W^2, Q^2) = \frac{Q^2 + m_0^2}{\Lambda^2(W^2)}, \quad (9)$$

where $\Lambda^2(W^2)$ increases slowly with energy and m_0 denotes a threshold mass, the distribution in the gluon momentum in the GVD/CDP is approximated[8, 9] by a δ -function situated at the average (or effective) gluon momentum determined by $\Lambda(W^2)$, i.e.

$$\tilde{\sigma}_{(q\bar{q})p}(\vec{l}_\perp^2, z, W^2) = \sigma^{(\infty)} \frac{1}{\pi} \delta(\vec{l}_\perp^2 - z(1-z)\Lambda^2(W^2)). \quad (10)$$

² In contrast to ref [8], we include the color factor $N_c = 3$ in the wave function squared.

The asymptotic value of the color dipole cross section (3), $\sigma^{(\infty)}$, turned out to be constant in good approximation[8]. The factor $z(1-z)$ in (10) is a model assumption that is particularly relevant at $Q^2 \gg m_0^2$. The energy dependence of $\Lambda^2(W^2)$ was parameterized[8], alternatively, by a power law or by a logarithm,

$$\Lambda^2(W^2) = \begin{cases} C_1(W^2 + W_0^2)^{C_2}, \\ C'_1 \ln\left(\frac{W^2}{W_0^2} + C'_2\right). \end{cases} \quad (11)$$

For later reference, we note the representation of the transverse and the longitudinal cross section (7) obtained upon substitution of (10) and upon having carried out all integrations except the one over \vec{k}_\perp^2 . In terms of the $q\bar{q}$ mass,

$$M^2 = \frac{\vec{k}_\perp^2}{z(1-z)}, \quad (12)$$

we find³

$$\sigma_{\gamma_T^* p}(W^2, Q^2) = \frac{\alpha R_{e^+e^-}}{3\pi} \sigma^{(\infty)} \cdot \int_{m_0^2} dM^2 \frac{1}{Q^2 + M^2} \left[\frac{M^2}{Q^2 + M^2} - \frac{1}{2} \left(1 + \frac{M^2 - \Lambda^2(W^2) - Q^2}{\sqrt{(M^2 + \Lambda^2(W^2) + Q^2)^2 - 4\Lambda^2(W^2)M^2}} \right) \right] \quad (13)$$

and

$$\sigma_{\gamma_L^* p}(W^2, Q^2) = \frac{\alpha R_{e^+e^-}}{3\pi} \sigma^{(\infty)} \cdot \int_{m_0^2} dM^2 \frac{1}{Q^2 + M^2} \left[\frac{Q^2}{Q^2 + M^2} - \frac{Q^2}{\sqrt{(M^2 + \Lambda^2(W^2) + Q^2)^2 - 4\Lambda^2(W^2)M^2}} \right]. \quad (14)$$

The total photoabsorption cross section, $\sigma_{\gamma^* p}(W^2, Q^2) = \sigma_{\gamma_T^* p} + \sigma_{\gamma_L^* p}$, scales in the variable η given by (9), i.e.

$$\sigma_{\gamma^* p}(W^2, Q^2) = \frac{\alpha R_{e^+e^-}}{3\pi} \sigma^{(\infty)} I^{(1)}(\eta), \quad (15)$$

with

$$\begin{aligned} I^{(1)}\left(\eta, \mu \equiv \frac{m_0^2}{\Lambda^2(W^2)}\right) \\ = \frac{1}{2} \ln \frac{\eta - 1 - \sqrt{(1+\eta)^2 - 4\mu}}{2\eta} + \frac{1}{2\sqrt{1+4(\eta-\mu)}} \\ \times \ln \frac{\eta(1 + \sqrt{1+4(\eta-\mu)})}{4\mu - 1 - 3\eta + \sqrt{(1+4(\eta-\mu))((1+\eta)^2 - 4\mu)}}, \end{aligned} \quad (16)$$

the dependence of $I^{(1)}$ on $m_0^2/\Lambda^2(W^2)$ being negligible for $m_0^2/\Lambda^2(W^2) \ll 1$. We also note the asymptotic form

$$\sigma_{\gamma^* p}(W^2, Q^2) = \frac{\alpha R_{e^+e^-}}{3\pi} \sigma^{(\infty)} \begin{cases} \ln(1/\eta), & \text{for } \eta \rightarrow m_0^2/\Lambda^2(W^2), \\ 1/2\eta, & \text{for } \eta \gg 1. \end{cases} \quad (17)$$

The agreement of the photoabsorption cross section with photoproduction for $Q^2 \rightarrow 0$ determines the product

$$R_{e^+e^-} \sigma^{(\infty)} = \sigma^{(\infty)} 3 \sum_f Q_f^2. \quad (18)$$

³ Here we ignore the additive ‘‘correction terms’’ [8] that assure an identical threshold mass, m_0 , for the incoming and outgoing $q\bar{q}$ pair in the forward Compton amplitude. The correction terms will be given below. For the transverse cross section, the correction is negligible, while in the longitudinal one, contributions are of the order of 10 %.

With three active quark flavors, $R_{e^+e^-} = 2$, we have $\sigma^{(\infty)} \cong 80\text{GeV}^{-2} \cong 31\text{ mb}$, while with four active flavors, $R_{e^+e^-} = 10/3$ and $\sigma^{(\infty)} \cong 48\text{GeV}^{-2} \cong 18.7\text{ mb}$ [8]. For further reference, we note the parameters entering the scaling variable η and the W dependence of $\Lambda^2(W^2)$, as determined by the fit to the total cross section [8]. For the power law in (11) we have

$$\begin{aligned} m_0^2 &= 0.16 \pm 0.01\text{GeV}^2, & W_0^2 &= 882 \pm 246\text{GeV}^2, \\ C_1 &= 0.34 \pm 0.05(\text{GeV}^2)^{1-C_2}, & C_2 &= 0.27 \pm 0.01, \end{aligned} \quad (19)$$

while for the logarithmic dependence,

$$\begin{aligned} m_0^2 &= 0.157 \pm 0.009\text{GeV}^2, & W_0'^2 &= 1015 \pm 334\text{GeV}^2, \\ C_1' &= 1.644 \pm 0.14\text{GeV}^2, & C_2' &= 4.1 \pm 0.04. \end{aligned} \quad (20)$$

We note that the GVD/CDP with scaling in η leads to the important conclusion [9] that

$$\lim_{\substack{W^2 \rightarrow \infty \\ Q^2 \text{ fixed}}} \frac{\sigma_{\gamma^*p}(W^2, Q^2)}{\sigma_{\gamma p}(W^2)} = 1, \quad (21)$$

i.e. virtual and real photons have the same cross section at infinite energy (“saturation”).

III. ELASTIC DIFFRACTION

We turn to diffractive production. The diagonal form (2) of $\sigma_{\gamma_{T,L}^*p}$ in transverse position space develops its full power when considering diffractive (forward) production, $\gamma^*p \rightarrow Xp$. Indeed, the diffractive production cross section of state X of spin 1 in the forward direction, via the two-gluon exchange generic structure ($x \rightarrow 0$) becomes [11],

$$\begin{aligned} & \left. \frac{d\sigma_{\gamma_{T,L}^*p \rightarrow Xp}(W^2, Q^2, t)}{dt} \right|_{t=0} \\ &= \frac{1}{16\pi} \int_0^1 dz \int d^2r_\perp \sum_{\lambda, \lambda'=\pm 1} |\psi_{T,L}^{(\lambda, \lambda')}(r_\perp, z, Q^2)|^2 \sigma_{(q\bar{q})p}^2(\vec{r}_\perp^2, z, W^2). \end{aligned} \quad (22)$$

The representation (22) contains the square of (the imaginary part⁴ of) the forward production amplitude for reaction (1) that enters (2) linearly and necessarily only involves $q\bar{q}$ pairs that couple to the photon and accordingly carry photon quantum numbers (“elastic diffraction”). The factor $1/16\pi$ in (22) stems from the application of the optical theorem when passing from the forward scattering amplitude of reaction (1) to the total cross section, $\sigma_{(q\bar{q})p}$. Diffractive production of higher spin states (inelastic diffraction) requires an additive term, $\sigma_{(q\bar{q})p}^2 \rightarrow \sigma_{(q\bar{q})p}^2 + \Delta\sigma_{(q\bar{q})p}^2$ in (22).

Note the close analogy of (22) to the simple ρ^0 dominance formula, where in photoproduction [13]

$$\left. \frac{d\sigma}{dt} \right|_{t=0} (\gamma p \rightarrow \rho^0 p) = \frac{1}{16\pi} \frac{\alpha\pi}{\gamma_\rho^2} \sigma_{\rho^0 p}^2. \quad (23)$$

The constant $\alpha\pi/\gamma_\rho^2$ denotes the photon- ρ^0 coupling strength as measured in e^+e^- -annihilation. The generalization (22) of (23) is an outgrowth of the diagonalization of the process $\gamma^*p \rightarrow Xp$ that is specific to the use of the variables \vec{r}_\perp and z . It is precisely with respect to these variables that the process $\gamma^*p \rightarrow Xp$ is truly elastic: a $q\bar{q}$ dipole being specified by \vec{r}_\perp and z and carrying photon quantum numbers undergoes elastic forward scattering.

Inserting the photon wave function (4) as well as the representation (3) for the dipole cross section into (22), we obtain the momentum space representation

$$\begin{aligned} & \left. \frac{d\sigma_{\gamma_{T,L}^*p \rightarrow Xp}(W^2, Q^2, t)}{dt} \right|_{t=0} = \frac{1}{16\pi} \frac{3}{16\pi^3} \int_0^1 dz \int d^2k_\perp \cdot \\ & \cdot \left[\int d^2l_\perp \tilde{\sigma}_{(q\bar{q})p}(\vec{l}_\perp^2, z, W^2) (\mathcal{M}_{T,L}(\vec{k}_\perp, z, Q^2) - \mathcal{M}_{T,L}(\vec{k}_\perp + \vec{l}_\perp, z, Q^2)) \right]^2. \end{aligned} \quad (24)$$

⁴ Neglecting a potential contribution from a real part to the $(q\bar{q})p$ forward scattering amplitude seems justified on phenomenological grounds from the empirical knowledge on photon- and hadron-induced reactions [2]. For a brief theoretical estimate of the (small) ratio of the real to imaginary part of the $(q\bar{q})p$ forward scattering amplitude with two-gluon-exchange interaction, compare with ref.[12].

We emphasize the distinctive difference between (7) and (24) with respect to the order in which the square of the integrand is taken and the integration over the transverse gluon momentum, \vec{l}_\perp , is performed.

Upon substituting (5) and (6) into (24), and upon carrying out angular integrations, with (10), the diffractive forward production by transverse photons becomes,

$$\left. \frac{d\sigma_{\gamma_T^* p \rightarrow Xp}}{dt} \right|_{t=0} = \frac{\alpha \cdot R_{e^+e^-}}{3 \cdot 16\pi^2} (\sigma^{(\infty)})^2 \int \frac{dM^2}{M^2} \cdot \left[\frac{M^2}{Q^2 + M^2} - \frac{1}{2} \left(1 + \frac{M^2 - \Lambda^2(W^2) - Q^2}{\sqrt{(M^2 + \Lambda^2(W^2) + Q^2)^2 - 4\Lambda^2(W^2)M^2}} \right) \right]^2, \quad (25)$$

while for longitudinal ones,

$$\left. \frac{d\sigma_{\gamma_L^* p \rightarrow Xp}}{dt} \right|_{t=0} = \frac{\alpha \cdot R_{e^+e^-}}{3 \cdot 16\pi^2} (\sigma^{(\infty)})^2 \cdot \int \frac{dM^2}{Q^2} \left[\frac{Q^2}{Q^2 + M^2} - \frac{Q^2}{\sqrt{(M^2 + \Lambda^2(W^2) + Q^2)^2 - 4\Lambda^2(W^2)M^2}} \right]^2. \quad (26)$$

The integrands in (25) and (26) yield the mass spectra, $d\sigma_{\gamma_{T,L}^* p \rightarrow Xp}/dtdM^2$, for diffractive forward production ($t \cong 0$) of states X of unit spin by transversely and longitudinally polarized photons, respectively.

Taking the sum of (25) and (26), one finds

$$\left. \frac{d\sigma_{\gamma^* p \rightarrow Xp}}{dt} \right|_{t=0} = \frac{\alpha R_{e^+e^-}}{3 \cdot 32\pi^2} (\sigma^{(\infty)})^2 \cdot \int \frac{dM^2}{M^2} \left[1 - \frac{(M^2 + Q^2)^2 - (M^2 - Q^2)\Lambda^2(W^2)}{(M^2 + Q^2)\sqrt{(M^2 + \Lambda^2(W^2) + Q^2)^2 - 4\Lambda^2(W^2)M^2}} \right]. \quad (27)$$

The integrand in (27) yields the mass spectrum for the case of unpolarized photons. Carrying out the integral in (27), we find the total elastic forward production cross section in the mass interval (M_1^2, M_2^2) ,

$$\left. \frac{d\sigma_{\gamma^* p \rightarrow Xp}^{(M_1^2, M_2^2)}}{dt} \right|_{t=0} = \frac{\alpha R_{e^+e^-}}{3\pi \cdot 16\pi} \cdot \Pi_0(Q^2, \Lambda^2(W^2), M^2) \Big|_{M_1^2}^{M_2^2} \quad (28)$$

with

$$\begin{aligned} \Pi_0(Q^2, \Lambda^2(W^2), M^2) &= \frac{1}{2} \ln \frac{(\Lambda^2 + Q^2)(\sqrt{X} + Q^2 + \Lambda^2) + M^2(Q^2 - \Lambda^2)}{\sqrt{X} + M^2 + Q^2 - \Lambda^2} - \\ &- \frac{\Lambda^2}{\sqrt{\Lambda^2(4Q^2 + \Lambda^2)}} \ln \frac{\sqrt{\Lambda^2(4Q^2 + \Lambda^2)}\sqrt{X} + \Lambda^2(3Q^2 - M^2 + \Lambda^2)}{Q^2 + M^2}, \end{aligned} \quad (29)$$

where the short-hand

$$X(M^2, Q^2, \Lambda^2(W^2)) \equiv (M^2 + \Lambda^2(W^2) + Q^2)^2 - 4\Lambda^2(W^2)M^2 \quad (30)$$

is being used and $\Lambda^2 \equiv \Lambda^2(W^2)$ in (29).

IV. THE SUM RULES

A comparison of the mass spectra in (25) and (26) with the expressions for the total cross section, $\sigma_{\gamma_{T,L}^* p}$, in (13) and (14) allows one to represent the total cross sections in terms of diffractive forward production, $\gamma^* p \rightarrow Xp$, of states X that carry photon quantum numbers (elastic diffraction). One finds the sum rules

$$\sigma_{\gamma_T^* p}(W^2, Q^2) = \sqrt{16\pi} \sqrt{\frac{\alpha R_{e^+e^-}}{3\pi}} \int_{m_0^2} dM^2 \frac{M}{Q^2 + M^2} \sqrt{\left. \frac{d\sigma_{\gamma_T^*}}{dtdM^2} \right|_{t=0}} \quad (31)$$

and

$$\sigma_{\gamma_{Lp}^*}(W^2, Q^2) = \sqrt{16\pi} \sqrt{\frac{\alpha R_{e^+e^-}}{3\pi}} \int_{m_0^2} dM^2 \frac{\sqrt{Q^2}}{Q^2 + M^2} \sqrt{\left. \frac{d\sigma_{\gamma_L^*}}{dt dM^2} \right|_{t=0}}. \quad (32)$$

For the unpolarized cross section, by taking the sum of (31) and (32), we have

$$\sigma_{\gamma^*p}(W^2, Q^2) = \sqrt{16\pi} \sqrt{\frac{\alpha R_{e^+e^-}}{3\pi}} \int_{m_0^2} dM^2 \frac{M}{Q^2 + M^2} \left[\sqrt{\left. \frac{d\sigma_{\gamma_T^*}}{dt dM^2} \right|_{t=0}} + \sqrt{\frac{Q^2}{M^2}} \sqrt{\left. \frac{d\sigma_{\gamma_L^*}}{dt dM^2} \right|_{t=0}} \right]. \quad (33)$$

In order to simplify the notation in (32) and (33), we have dropped the arguments W^2 , Q^2 , t and M^2 the diffractive production cross sections $d\sigma_{\gamma_{T,Lp}^*}/dM^2 dt$ depend on. We stress that the sum rules (31) to (33) follow from the two-gluon exchange structure of QCD that is contained in the representation of the cross sections (2) and (22) in conjunction with the form (3) of the color-dipole cross section. The δ -function ansatz (10) for the gluon-momentum distribution, also used in the above derivation of the sum rules, does not introduce much loss of generality. It is suggested and supported by the empirical scaling in η ; the gluon transverse momentum is fixed to coincide with its average or effective value determined by $\Lambda^2(W^2)$ [9].

It is amusing to note that (33) is the GVD analogue of the photoproduction sum rule from vector meson dominance [13]

$$\sigma_{\gamma p}(W^2) = \sum_{V=\rho^0, \omega, \phi, \dots} \sqrt{16\pi} \sqrt{\frac{\alpha\pi}{\gamma_V^2}} \sqrt{\left. \frac{d\sigma_{\gamma p \rightarrow V_0}}{dt} \right|_{t=0}}. \quad (34)$$

Indeed, multiplying the (imaginary part of the) amplitude for $\gamma^*p \rightarrow Xp$ by the propagator factor $M^2/(Q^2 + M^2)$ and a factor $1/M$ for the strength of the photon coupling normalized by $\sqrt{\alpha \cdot R_{e^+e^-}/3\pi}$, implies (31).⁵ An additional well-known factor of $\sqrt{Q^2/M^2}$ [15] is needed for the longitudinal cross section in (32). Note that this derivation of the sum rules (31) to (33) is dependent on the production mechanism for $\gamma^*p \rightarrow Xp$ in so far only, as the Q^2 dependence induced by the transition from the timelike four momentum squared, $P_X^2 = M^2$, of the final state X to the spacelike four momentum squared, Q^2 , of the virtual photon coupled to X is assumed to be fully contained in the aforementioned (propagator) factors. In other words, it is assumed that the underlying transition from the timelike to spacelike four momenta with respect to the vector state X does not affect $d\sigma_{\gamma_{T,Lp}^*}/dM^2 dt$ at $t = 0$. This condition is fulfilled in the GVD/CDP based on (2), (3) and (22) with (10).

The above derivation of the sum rules (31) to (33), based on the comparison of the QCD-based mass spectra for elastic diffraction in (25) and (26) with the ones for $\sigma_{\gamma_{T,Lp}^*}$ in (13) and (14), demonstrates explicitly that the QCD-based color-dipole picture implies GVD for low- x DIS. The terminology GVD/CDP for our approach to DIS at low x is appropriate.

The experimental validity of the photoproduction sum rule (34) was carefully investigated in the late sixties and the early seventies[16]. Insertion of the experimental data for the total photoproduction cross section on the left-hand side in (34), and of the cross sections for vector meson forward production on the right-hand side, revealed a discrepancy of 22 % that led to the formulation of generalized vector dominance[3]. A recent experimental test of (34) at HERA energies was presented in ref. [17].

An analogous direct experimental test of the sum rules (31) to (33) for virtual photons is more difficult to be carried out. The diffractive forward production cross sections in (22) and (31) to (33) refer to the production of spin 1 (vector) states; otherwise the produced states would never couple to the photon and build up the imaginary part of the (virtual) forward Compton scattering amplitude. A direct experimental verification of (31) to (33), accordingly, requires the projection of the spin 1 component contained in the diffractively produced state X of mass M . In addition, diffractive production by transverse and longitudinal photons has to be separated; an assumption of s-channel helicity conservation[15], as in vector meson production, may be helpful, as long as no direct separation of production by transverse and longitudinal photons will be available.

⁵ Based on this GVD argument, the sum rule (31) was indeed given before[14].

We note that, independently of their direct experimental verification, the sum rules (31) to (33) are of theoretical interest. They most explicitly demonstrate that (22) (containing a dipole cross section, $\sigma_{(q\bar{q})p}$, identical to the one in σ_{γ^*p} in (2)) describes *elastic* diffraction, elastic with respect to the photon quantum numbers carried by the incoming and outgoing $q\bar{q}$ states; had the diffractively produced state X quantum numbers different from the ones of the photon, e.g. a different spin, the sum rules (31) to (33) could never be valid. In order to incorporate *inelastic* diffraction, the dipole cross section in the expression for diffractive production (22) has to be replaced by the addition of a term describing inelastic diffraction.

V. COMPARISON WITH EXPERIMENTAL RESULTS ON DIFFRACTIVE PRODUCTION

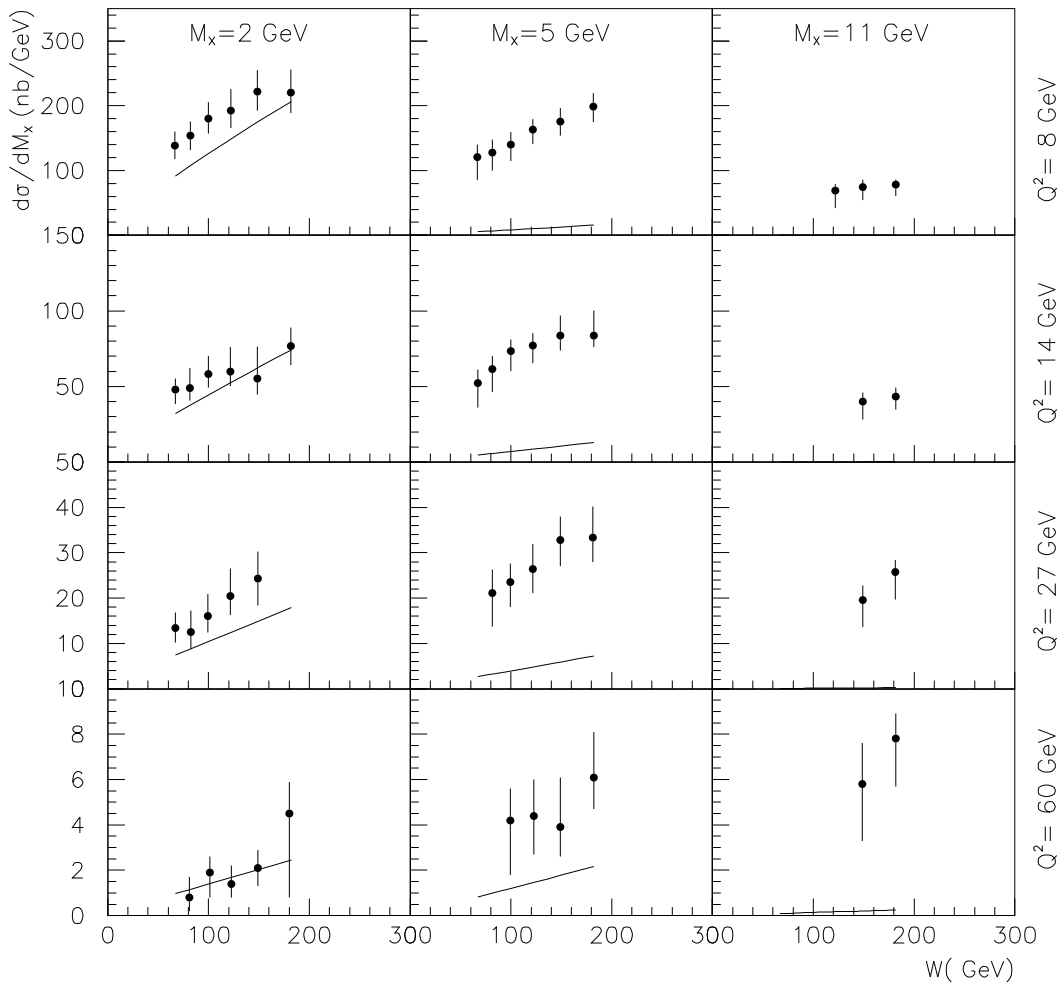


FIG. 1: The ZEUS data for diffractive production, $\gamma^*p \rightarrow Xp$, as a function of the energy, W , for different masses M_X and photon virtuality Q^2 compared with the GVD/CDP predictions for elastic diffraction. The excess of the data with respect to theory is due to diffractive production of states X of mass M_X that do not couple to the photon, and accordingly cannot contribute to the (virtual) forward Compton amplitude that builds up the total cross section, σ_{γ^*p} .

We turn to a comparison of our results on elastic diffractive production with the experimental data. The ZEUS collaboration has presented data [18] for the mass distribution integrated over the distribution in momentum transfer t . Assuming an exponential behavior, $\exp(-bt)$, the experimental data on $d\sigma_{\gamma^*p \rightarrow Xp}/dM_X$ are related to the mass

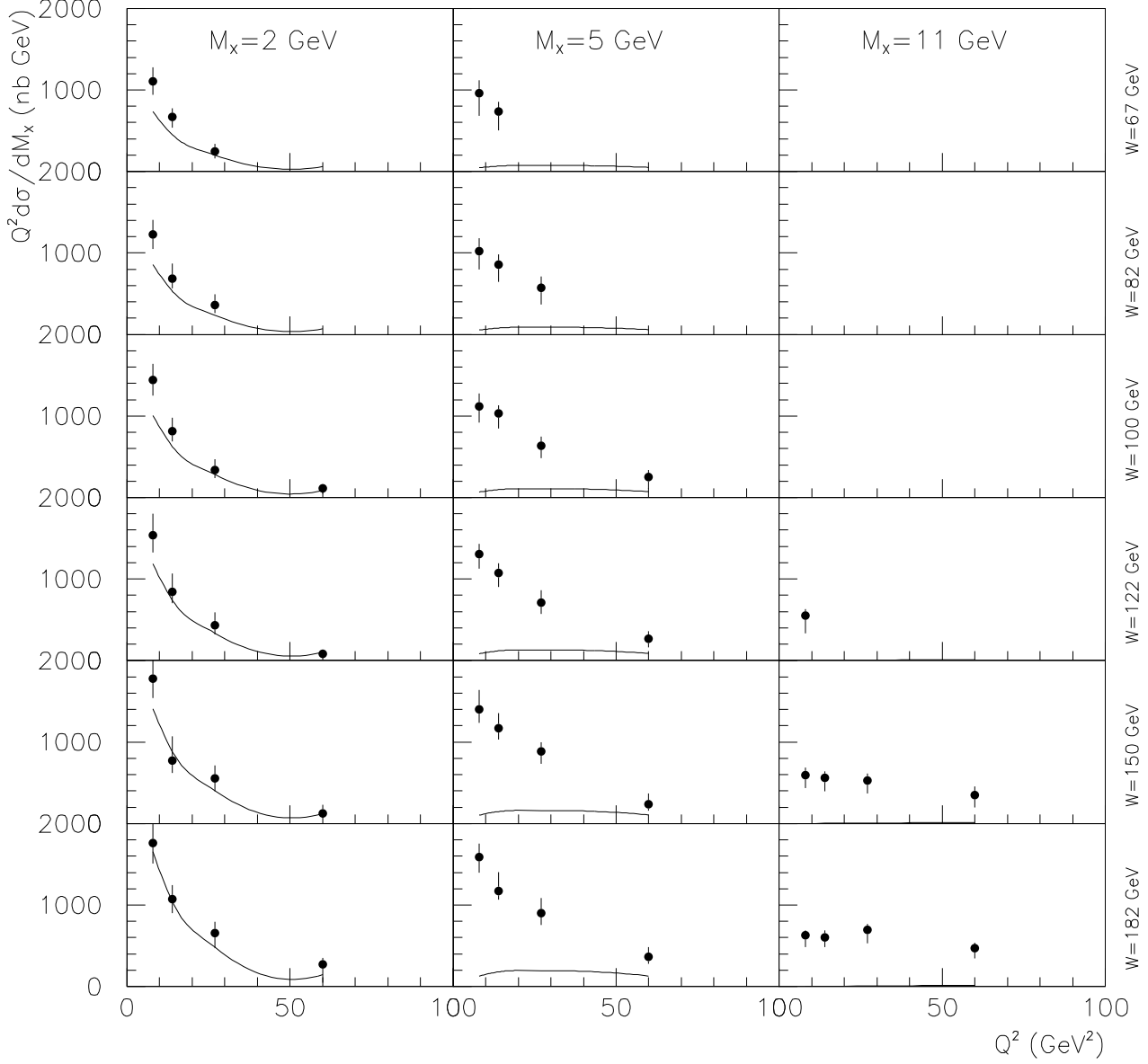


FIG. 2: As in fig. 1, but for $Q^2 d\sigma_{\gamma^*p \rightarrow Xp}/dM_X$ as a function of Q^2 for different masses M_X .

spectrum in the integrand of (27) by

$$\frac{d\sigma_{\gamma^*p \rightarrow Xp}}{dM_X} = 2M_X \int dt e^{-bt} \left. \frac{d\sigma_{\gamma^*p \rightarrow Xp}}{dt dM_X^2} \right|_{t=0} = \frac{2M_X}{b} \left. \frac{d\sigma_{\gamma^*p \rightarrow Xp}}{dt dM_X^2} \right|_{t=0}. \quad (35)$$

In (35), we use the notation of the ZEUS collaboration by the replacement $M \rightarrow M_X$. In fig. 1, following the representation of the data by the ZEUS collaboration, we show the energy dependence of $d\sigma_{\gamma^*p \rightarrow Xp}/dM_X$ for various masses M_X and various fixed values of $Q^2 = 8\text{GeV}^2$ to $Q^2 = 60\text{GeV}^2$. As in the total cross section (15), in (27) and

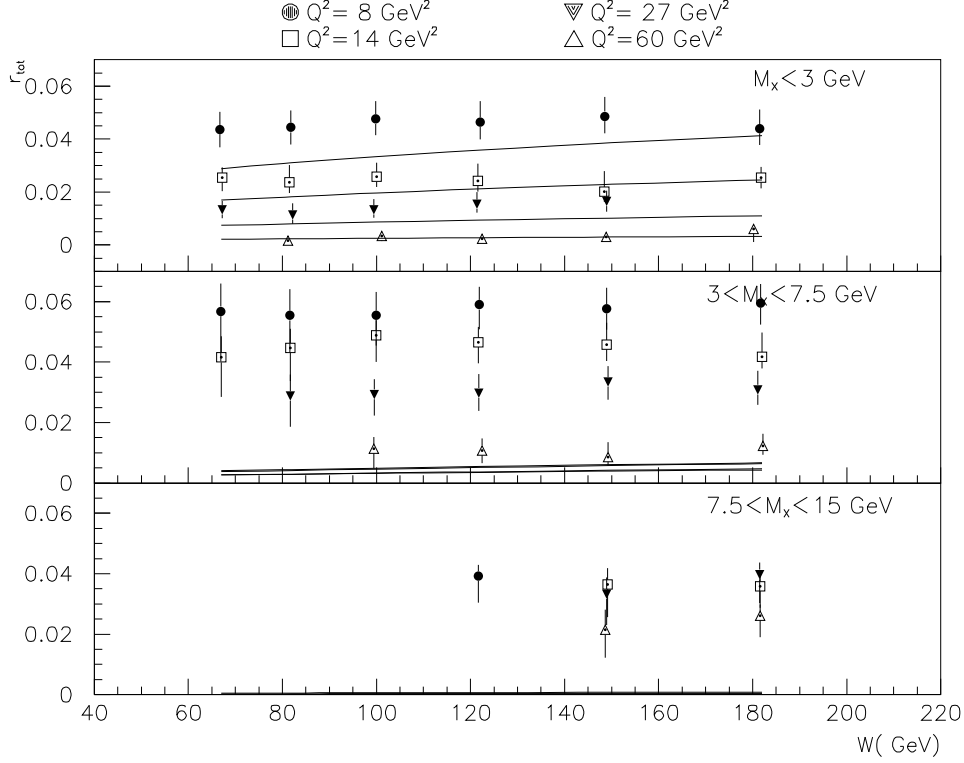


FIG. 3: The ratio of the cross section for diffractive production to the total cross section as a function of the energy, W , for different values of M_X and Q^2 . The theoretical curves, as in figs. 1,2, show the predictions from the GVD/CDP for the component of diffraction that saturates the imaginary part of the virtual forward Compton amplitude (elastic diffraction).

(35), we have used⁶ $R_{e^+e^-} = 10/3$ as well as $\sigma^{(\infty)} = 48\text{GeV}^{-2}$, and⁷

$b = 7.5\text{GeV}^{-2}$. Figure 1 shows that diffractive production at low masses is approximately described by elastic diffraction, i.e. by diffractive production of those spin 1 states that saturate the (imaginary part of the virtual) Compton forward scattering amplitude. For the higher masses of $M_X = 5\text{GeV}$ and $M_X = 11\text{GeV}$, as expected, elastic diffraction does by no means fully represent the diffractive cross section. The discrepancy between theory and experiment decreases with increasing Q^2 , however, i.e. with increasing $\beta \equiv Q^2/(Q^2 + M_X^2)$. In fig. 2, we show the Q^2 dependence in a plot of $Q^2 d\sigma_{\gamma^*p \rightarrow X_p}/dM_X$ against Q^2 . As anticipated from fig. 1, for $M_X = 2\text{GeV}$ there is reasonable consistency between the theoretically calculated production of spin 1 states and the experimental data.

⁶ The total cross section is equally well represented in the three-flavour option, $R_{e^+e^-} = 2$ but $\sigma^{(\infty)} = 80\text{GeV}^{-2}$. In this case, $b = 12.5\text{GeV}^{-2}$ is to be used.

⁷ A detailed analysis of the effect of a potential Q^2 or M^2 dependence of the slope parameter seems somewhat premature in view of the available data and the incompleteness of the theory with respect to inelastic diffraction.

In fig. 3, we show the ratio

$$r_{\text{tot}} = \frac{\int_{M_a}^{M_b} dM_X d\sigma_{\gamma^*p \rightarrow Xp}/dM_X}{\sigma_{\gamma^*p}} \quad (36)$$

as a function of the energy W . As anticipated from the previous figures, there is some discrepancy in normalization and also in energy dependence. Note, however, that the energy dependence, as a consequence of the different structure of the expressions for σ_{γ^*p} in (7) and for $d\sigma_{\gamma^*p \rightarrow Xp}/dt$ in (24), is quite similar. The naive expectation (15) that the linearity with respect to the dipole cross section in the total cross section (2) and the non-linearity in the diffractive production cross section (22) lead to distinctly different energy dependences is not valid.

The substantial excess of the cross section $d\sigma_{\gamma^*p \rightarrow Xp}/dM_X$ for $M_X = 5\text{GeV}$ and $M_X = 11\text{GeV}$ is due to the production of states that do not couple to the photon and accordingly do not contribute to the imaginary part of the virtual forward Compton scattering amplitude (inelastic diffraction). From the thrust and sphericity analysis of the diffractively produced states [1], we know that these predominantly consist of hadronized $q\bar{q}$ states with some (fairly small) admixture of a $q\bar{q} + \text{gluon}$ component. The excess in $d\sigma_{\gamma^*p \rightarrow Xp}/dM_X$ must be associated with states of spin higher than the photon spin. With increasing Q^2 , due to propagator effects, the relative contribution of low masses becomes increasingly more suppressed, the diffraction process becomes more elastic. The discrepancy between our theoretical curves and the experimental data is decreased at high Q^2 , or, in terms of the frequently employed variable $\beta = Q^2/(Q^2 + M_X^2)$, elastic diffraction becomes dominant for $\beta \rightarrow 1$.

Any theory of high-mass (small β) diffraction has to obey the constraint that the component needed in addition to the elastic one be truly inelastic in the sense of being unable to contribute to the imaginary part of the forward Compton scattering amplitude. After all, the forward Compton amplitude is saturated by the elastic component which contributes the amount to diffractive production that is shown in figs. 1 to 3. It is worth stressing again the fairly general validity of the sum rules (31) to (33), this saturation property is based on.

Some recent theoretical work [19, 20, 21] on diffractive production of large masses, i.e. $\beta \ll 1$, concentrated on adding a quark-antiquark-gluon ($q\bar{q}g$) component to the $q\bar{q}$ wave function of the photon. Even though the data on diffractive production are accounted for, this approach suffers from a serious inconsistency, as, without justification, the additional $q\bar{q}g$ component is only taken into account in the photon wave function entering diffractive production (i.e. in (22)), while being ignored in the total cross section (i.e. in (2)), thus disregarding the optical theorem. From a theoretical point of view, the interplay of $q\bar{q}$ and $q\bar{q}g$ components in the wave function for diffractive production and the total cross section is analyzed in [22]. The approach of ref.[22] treats the $q\bar{q}$ and $q\bar{q}g$ components of the photon on equal footing. It does not contain a truly inelastic component. Accepting a universal (model-independent) validity of the sum rules in Section 4, an approach purely based on an elastic component that describes diffractive production is likely to fail for the total cross section. Indeed, inserting an amplitude for diffractive production into the sum rules that coincides with experiment, the resulting total cross section is likely to disagree with experiment, since agreement with experiment is achieved by the much smaller amplitude for elastic diffractive production by itself. A clear discrimination between elastic and inelastic diffractive production is made right from the outset in the color-dipole approach of [23]. It is not entirely clear from the presentation in [23] by what means a potential contribution of the “inelastic” component to the imaginary part of the virtual forward Compton scattering amplitude is excluded.

VI. IMPLICATIONS FOR σ_{γ^*p}

In view of the comparison of our results for elastic diffraction with the experimental data, it will be enlightening to return to the theoretical description of the total cross section, σ_{γ^*p} . The strong decrease of the theoretical results for elastic diffractive production with increasing mass, $M \equiv M_X$, by no means implies that contributions due to large masses in the integral representations (13) and (14), or, equivalently, (31) and (32), for the transverse and longitudinal total cross sections become negligible. This may be explicitly seen by evaluating the integral representations as a function of an upper limit, m_1^2 . Indeed, the sum rules (31) and (32) suggest this upper limit to be approximately given by the upper end of the diffractively produced spectrum of masses.

The integration of (13) and (14) then yields

$$\begin{aligned} \sigma_{\gamma_T^*p} = & \frac{\alpha R_{e^+e^-}}{3\pi} \sigma^{(\infty)} \left[\frac{Q^2}{Q^2 + M^2} + \frac{1}{2} \ln \frac{Q^2 + M^2}{\sqrt{X} + Q^2 + M^2 - \Lambda^2} \right. \\ & \left. - \frac{2Q^2 + \Lambda^2}{2\sqrt{\Lambda^2(\Lambda^2 + 4Q^2)}} \ln \frac{\sqrt{\Lambda^2(\Lambda^2 + 4Q^2)X} + \Lambda^2(3Q^2 - M^2 + \Lambda^2)}{Q^2 + M^2} \right] \Bigg|_{m_0^2}^{m_1^2} \end{aligned} \quad (37)$$

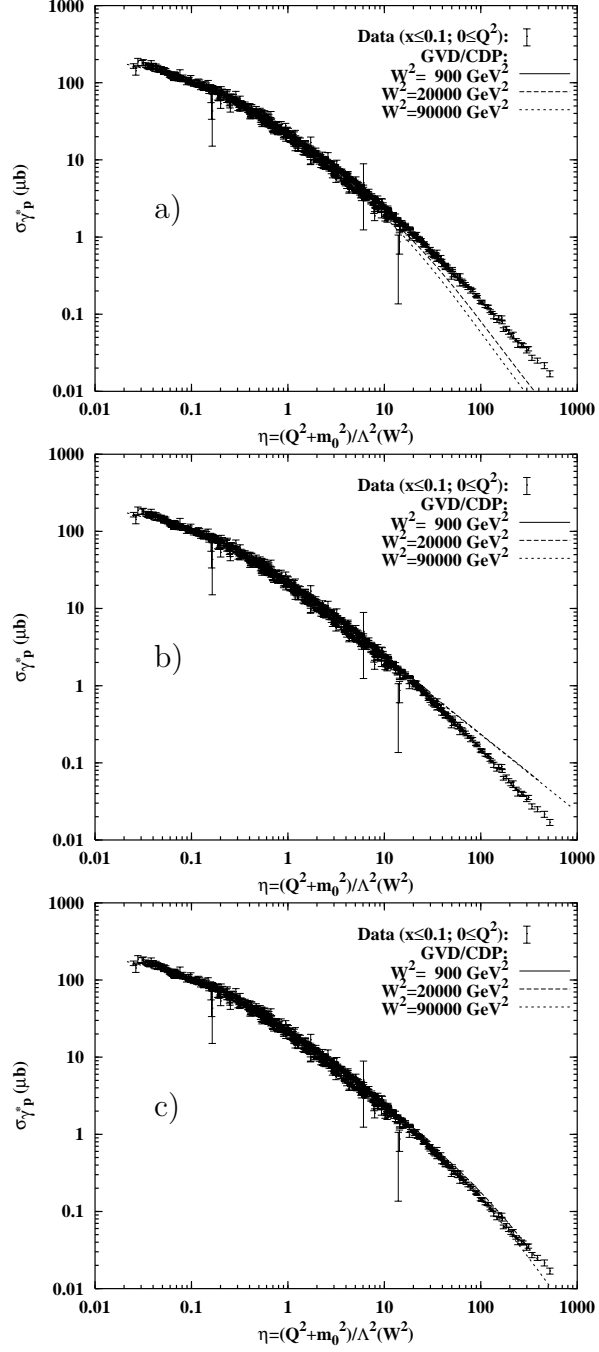


FIG. 4: The data for the total photoabsorption cross section, σ_{γ^*p} , as a function of the scaling variable η compared with the GVD/CDP predictions obtained for different values of the upper bound, m_1^2 , on the diffractive mass spectrum that is integrated over in the imaginary part of the virtual forward Compton scattering amplitude describing σ_{γ^*p} . Figures 4a to 4c refer to $m_1^2 = 100 \text{ GeV}^2$, $m_1^2 = \infty$ and $m_1^2 = 484 \text{ GeV}^2$, respectively.

and

$$\begin{aligned} \sigma_{\gamma_L^*p} = & \frac{\alpha R_{e^+e^-}}{3\pi} \sigma^{(\infty)} \left[\frac{-Q^2}{Q^2 + M^2} \right. \\ & \left. + \frac{Q^2}{\sqrt{\Lambda^2(\Lambda^2 + 4Q^2)}} \ln \frac{\sqrt{\Lambda^2(\Lambda^2 + 4Q^2)} X + \Lambda^2(3Q^2 - M^2 + \Lambda^2)}{Q^2 + M^2} \right] \Bigg|_{m_0^2}^{m_1^2}, \end{aligned} \quad (38)$$

where $\Lambda^2(W^2)$ is given in (11), and $X(M^2, Q^2, \Lambda^2(W^2))$ is defined in (30). The sum of (37) and (38), for $m_1^2 = \infty$, reduces to (16). For completeness, we also give the previously mentioned correction terms that have to be added to (13) and (14) as well as to (37) and (38), in order to assure identical lower limits, m_0^2 , in the initial and the final state of the (virtual) Compton forward scattering amplitude. The expressions given for these terms in ref. [8] may be simplified to become one-dimensional integrals that are to be carried out numerically. For the realistic case of $\Lambda^2 > 4m_0^2$, one finds,

$$\Delta\sigma_{\gamma_{Tp}^*} = \frac{\alpha R_{e^+e^-}}{6\pi} \sigma^{(\infty)} \int_{(\Lambda-m_0)^2}^{(\Lambda+m_0)^2} dM^2 \frac{1}{(Q^2 + M^2)} \quad (39)$$

$$\left[\frac{1}{2\pi} \arccos\left(\frac{\Lambda^2 + M^2 - m_0^2}{2M\Lambda}\right) + \frac{M^2 - \Lambda^2 - Q^2}{\pi\sqrt{X}} \arctan\sqrt{Y} \right],$$

and

$$\Delta\sigma_{\gamma_{Lp}^*} = \frac{\alpha R_{e^+e^-}}{6\pi} \sigma^{(\infty)} \int_{(\Lambda-m_0)^2}^{(\Lambda+m_0)^2} dM^2 \frac{1}{(Q^2 + M^2)} \cdot \frac{2}{\pi\sqrt{X}} \arctan\sqrt{Y}, \quad (40)$$

where

$$Y \equiv \frac{(M + \Lambda)^2 + Q^2}{(M - \Lambda)^2 + Q^2} \cdot \frac{m_0^2 - (M - \Lambda)^2}{(M + \Lambda)^2 - m_0^2}. \quad (41)$$

A comparison of the theoretical results for σ_{γ^*p} for different values of the upper limit, m_1^2 , with the experimental data [24, 25, 26, 27, 28] is shown in fig. 4. We emphasize that the experimental data cover the full range of the kinematic variables ($x < 0.1$, all Q^2 , including $Q^2 = 0$) where scaling in η was established in a model-independent analysis[8]. The results in fig. 4 are quite remarkable. They show that

- i) a restriction of m_1^2 to values (e.g. $m_1^2 = 100 \text{ GeV}^2$) below the upper limit of the mass where appreciable diffractive production was observed experimentally, leads to values of σ_{γ^*p} that for $\eta \geq 10$ lie much below the experimental scaling curve, i.e. a non-vanishing elastic diffractive production of large masses M_X is necessary for saturation of the forward Compton amplitude, even though
- ii) the previously used [8, 9] value of $m_1^2 = \infty$, for $\eta \gtrsim 10$ leads to results that lie above the experimental data.

The highest mass bin where appreciable diffractive production occurs, according to the results [1] from the ZEUS collaboration, is given by $M_X = 22 \text{ GeV}$. Accordingly we use

$$m_1^2 \simeq (22 \text{ GeV})^2 = 484 \text{ GeV}^2 \quad (42)$$

that yields good agreement with the experimental data for $\sigma_{\gamma^*p}(\eta)$ in the full kinematic range of $x \leq 0.1$, all Q^2 including $Q^2 = 0$, where scaling in η was established in a model-independent analysis of the experimental data.

The fact that an upper limit for the diffractively produced mass should enter the forward Compton amplitude at finite energy, W , is not unexpected. It is gratifying that its value (42) of $m_1 = 22 \text{ GeV}$, coincides with the upper limit of the range of masses where diffractive production, $\gamma^*p \rightarrow Xp$, is experimentally found to occur. Beyond that mass, inclusion of the mass spectrum from the GVD/CDP overestimates the total cross section, σ_{γ^*p} . This deficiency, in an approximate and admittedly somewhat crude manner, is repaired by restricting the range of integration by the upper limit in (42). The deviation from scaling in η resulting from the introduction of this upper limit is a fairly mild one.

VII. CONCLUSION

We summarize as follows:

- i) Our ansatz for DIS at low x that is based on the generic structure of two-gluon exchange from QCD supplemented by the empirical scaling behavior $\sigma_{\gamma^*p} = \sigma_{\gamma^*p}(\eta)$ leads to sum rules that explicitly express σ_{γ^*p} as an appropriate integral over the square root of the elastic diffractive forward production cross section. The agreement of the expression for σ_{γ^*p} with the experimental data explicitly demonstrates that DIS at low x is understood in terms of diffractive forward scattering of massive $q\bar{q}$ pairs on the nucleon (GVD/CDP).

- ii) A comparison of the theoretical results for elastic diffractive production, i.e. the production of states X in $\gamma^*p \rightarrow Xp$ that carry photon quantum numbers, is the dominant mechanism for $\beta \equiv Q^2/(Q^2 + M_X^2) \rightarrow 1$. The excess of the experimental data with respect to elastic diffraction observed for $\beta \ll 1$ is attributed to inelastic diffraction, i.e. to the production of states X that do not carry photon quantum numbers and are not contributing to the imaginary part of the virtual Compton forward scattering amplitude.
- iii) The connection between the total photoabsorption cross section and diffractive production suggests an extension of the kinematic range, in which the total photoabsorption cross section, σ_{γ^*p} , is represented by the GVD/CDP. This range now includes the full kinematic region where scaling in η holds, $x \leq 0.1$ and all $Q^2 \geq 0$.
- iv) Any serious theoretical model for diffractive production must be examined with respect to its compatibility with the experimental data for the total virtual photoabsorption cross section that is related to (elastic) diffraction via the optical theorem.

Acknowledgement

One of the authors (D.S.) thanks the MPI in Munich, where this work was finalized, for warm hospitality and C. Kiesling and L. Stodolsky for useful discussions. The support by M. Tentyukov in the presentation of the data is gratefully acknowledged.

-
- [1] The ZEUS collaboration, S. Chekanov et al., DESY-01-097 (2001).
 - [2] L. Stodolsky, Phys. Rev. Lett. **22**, 973 (1967);
D. Leith, in “Electromagnetic Interactions of Hadrons”, ed. by A. Donnachie and G. Shaw, Plenum Press (New York 1978) p.345.
 - [3] J.J. Sakurai and D. Schildknecht, Phys. Lett. **40B**, 121 (1972);
B. Gorceyca, D. Schildknecht, Phys. Lett. **47B**, 71 (1973).
 - [4] F.E. Low, Phys. Rev. D **12**, 163 (1975);
S. Nussinov, Phys. Rev. Lett. **34**, 1286 (1975); Phys. Rev. D **14**, 246 (1976);
J. Gunion, D. Soper, Phys. Rev. D **15**, 2617 (1977).
 - [5] N.N. Nikolaev, B.G. Zakharov, Z. Phys. C **49**, 607 (1991).
 - [6] H. Fraas, B.J. Read and D. Schildknecht, Nucl. Phys. B **86**, 346 (1975);
R. Devenish, D. Schildknecht, Phys. Rev. D **19**, 93 (1976).
 - [7] L. Frankfurt, V. Guzey, M. Strikman, Phys. Rev. D **58**, 094039 (1998).
 - [8] D. Schildknecht, at “Diffraction2000”, Cetraro, Italy, September 2-7, 2000, Nucl. Phys. B Proc. Suppl. **B99**, 121 (2001);
D. Schildknecht, B. Surrow, M. Tentyukov, Phys. Lett. B **499**, 116 (2001);
G. Cvetic, D. Schildknecht, B. Surrow, M. Tentyukov, Eur. Phys. J. C **20**, 77 (2001).
 - [9] D. Schildknecht, B. Surrow, M. Tentyukov, Mod. Phys. Lett. A, Vol.16 (2001) 1829.
 - [10] D. Schildknecht and M. Tentyukov, BI-TP 2002/04, hep-ph/0203028
 - [11] N.N. Nikolaev, B.G. Zakharov, Z. Phys. C **53**, 331 (1992).
 - [12] E.M. Levin, A.D. Martin, M.G. Ryskin and T. Teubner, Z. Phys. C **74**, 671 (1997).
 - [13] L. Stodolsky, Phys. Rev. Lett. **18**, 135 (1967);
H. Joos, Phys. Lett. **B24**, 103 (1967).
 - [14] D. Schildknecht, H. Spiesberger, Acta Physica Pol. **B29**, 1261 (1998).
 - [15] H. Fraas and D. Schildknecht, Nucl. Phys. B **14**, 543 (1969).
 - [16] G. Wolf, in Proc. of the 1971 Internat. Symp. on Electron and Photon Interactions at High Energies, ed. by N.B. Mistry, Cornell Univ. (1972).
 - [17] The ZEUS collaboration, S. Chekanov et al., DESY-01-216 (2001).
 - [18] The ZEUS collaboration, J. Breitweg et al., Eur. Phys. J. C **6**, 43 (1999).
 - [19] K. Golec-Biernat, M. Wüsthoff, Phys. Rev. D **60**, 114023 (1999).
 - [20] J.R. Forshaw, G.R. Kerley, G. Shaw, hep-ph/9910251 (1999).
 - [21] J. Bartels, J. Ellis, H. Kowalski, M. Wüsthoff, hep-ph/9803497.
 - [22] N.N. Nikolaev, B.G. Zakharov, Z. Phys. C **64**, 631 (1994).
 - [23] A. Bialas, R. Peschanski, Ch. Royon, Phys. Rev. D **57**, 6899 (1998);
A. Bialas, R. Peschanski, Phys. Lett. **B387**, 405 (1996);
A. Bialas, R. Peschanski, Phys. Lett. **B378**, 302 (1996).
 - [24] ZEUS 96/97: S. Chekanov et al., ZEUS collab., DESY-01-014, submitted to Eur. Phys. J. C; M. Derrick et al., Z. Phys. C **72**, 399 (1996); ZEUS SVTX 95: J. Breitweg et al., ZEUS collab., Euro. Phys. J. C **7**, 609 (1999); ZEUS BPC 95f: J.

- Breitweg et al., ZEUS collab., Phys. Lett. B407, 432 (1997); ZEUS BPT 97: J. Breitweg et al., ZEUS collab., Phys. Lett. B487, 53 (2000).
- [25] H1 SVTX 95: C. Adloff et al., H1 collab., Nucl. Phys. B497, 3 (1997); H1 96/97: C. Adloff et al., H1 collab., Euro. Phys. J. C21, 33 (2001); H1 97: C. Adloff et al., H1 collab., Euro. Phys. J. C13, 609 (2000).
- [26] E665 Collaboration, Adams et al., Phys. Rev D54, 3006 (1996).
- [27] NMC Collaboration, Arneodo et al., Nucl.Phys. B483, 3 (1997).
- [28] BCDMS Collaboration, Benvenuti et al., Phys. Lett. B223, 485 (1989).